Stable states with nonzero entropy under broken $\mathcal{PT}$ symmetry

Jingwei Wen [1], Chao Zheng,[2] Zhangdong Ye [1], Tao Xin,[3,4,*] and Guilu Long[1,5,6,7,†]

[1]*State Key Laboratory of Low-Dimensional Quantum Physics and Department of Physics, Tsinghua University, Beijing 100084, China*
[2]*Department of Physics, College of Science, North China University of Technology, Beijing 100144, China*
[3]*Shenzhen Institute for Quantum Science and Engineering, Southern University of Science and Technology, Shenzhen 518055, China*
[4]*Guangdong Provincial Key Laboratory of Quantum Science and Engineering, Southern University of Science and Technology,*
Shenzhen 518055, Guangdong, China
[5]*Frontier Science Center for Quantum Information, Beijing 100084, China*
[6]*Beijing National Research Center for Information Science and Technology, Beijing 100084, China*
[7]*Beijing Academy of Quantum Information Sciences, Beijing 100193, China*

The $\mathcal{PT}$-symmetric non-Hermitian systems have been widely studied and explored both in theory and in experiment due to their various interesting features. In this work we focus on the dynamical features of a triple-qubit system, one of which evolves under a local $\mathcal{PT}$-symmetric Hamiltonian. An abnormal dynamic pattern in the entropy evolution process is identified that presents a parameter-dependent stable state, determined by the non-Hermiticity of Hamiltonian in the broken phase of $\mathcal{PT}$ symmetry. The entanglement and mutual information of a two-body subsystem can increase beyond the initial values, which do not exist in the Hermitian and two-qubit $\mathcal{PT}$-symmetric systems. Moreover, an experimental demonstration of the stable states in non-Hermitian systems with nonzero entropy and entanglement is realized on a four-qubit quantum simulator with nuclear spins. Our work reveals the distinctive dynamic features in the triple-qubit $\mathcal{PT}$-symmetric system and paves the way for practical quantum simulation of multiparty non-Hermitian system on quantum computers.

I. INTRODUCTION

In the conventional quantum mechanics, the Hamiltonian of a closed system requires it to be Hermitian [1], which guarantees the reality of the energy spectrum and the unitarity of the corresponding time evolution operators. However, the Hermiticity requirement is a sufficient condition but not necessary for real eigenvalues, and in 1998 [2], Bender and Boettcher found that a class of Hamiltonians satisfying joint $\mathcal{P}$ (spatial reflection) and $\mathcal{T}$ (time reversal) symmetry instead of Hermiticity can still have real eigenvalues in the unbroken phase [3,4]. Moreover, there exists a critical point for phase transition from the $\mathcal{PT}$ unbroken phase to a broken phase, called the exceptional point or branch point [5–7]. Because of various peculiar characters in this kind of non-Hermitian system, such as the violation of the no-signaling principle [8,9], entanglement restoration [10,11], and reversible-irreversible criticality in information flow [12,13], the $\mathcal{PT}$-symmetric quantum mechanics has aroused continuous attention and research interests in many directions. Recently, there has been

some related research on its potential applications in reconstructing standard quantum theory [14,15], and it has been shown that a unitary evolution can be introduced by redefining the inner product of quantum states [16,17], which makes it equivalent to the Hermitian quantum theory.

In experimentation, many quantum processes such as symmetry-breaking transitions [18–22], observation of exceptional points [23,24], and topological features [25,26] of the $\mathcal{PT}$-symmetric system have been demonstrated, and they depend mainly on the optical systems [13], nuclear spins [11,27], ultracold atoms [18], nitrogen-vacancy centers [19], and superconductor systems [23] by introducing balanced gain and loss or state-selective dissipation. Moreover, some previous research [9,11] focuses on the two-body non-Hermitian system as shown in Fig. 1, where two qubits (Alice and Bob) are entangled initially and one of them (Alice) evolves under a local $\mathcal{PT}$-symmetric Hamiltonian. Such a two-qubit model can lead to oscillations of entropy and entanglement in the unbroken phase of $\mathcal{PT}$ symmetry, which violates the property of entanglement monotonicity [10,11]. Specifically, the entropy and entanglement of both qubits will decay exponentially to zero in the broken phase and form stable states which do not vary with time. Such stable states, whose dynamic process is named a normal dynamic pattern (NDP) here, are related only to the quantum phase but are independent of the degree of non-Hermiticity.

However, in this work we find that when the system is extended from a two-body to a triple-body model, another kind of evolution process, named an abnormal dynamic
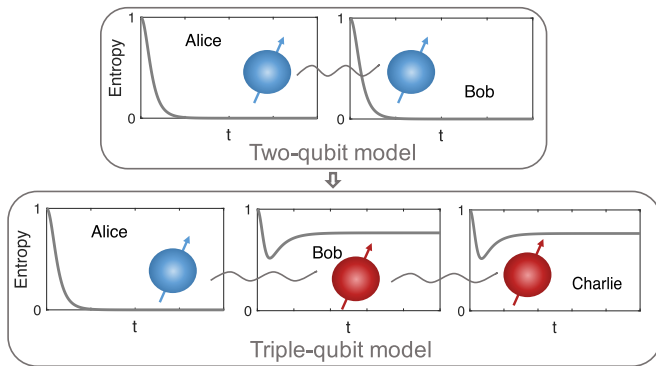
FIG. 1. The multiqubit system with local $\mathcal{PT}$-symmetric operators. A quantum system is initialized as a maximally entangled state and the first qubit (Alice) undergoes a local $\mathcal{PT}$-symmetric operation, while the other qubits remain isolated. The black lines are entropy evolution with time in a broken $\mathcal{PT}$-symmetric phase.

pattern (ADP) here, rises up. Subsystems evolving under ADP can present novel non-Hermiticity-related stable states with nonzero entropy. By controlling the local system of Alice, the entanglement and mutual information between Bob and Charlie can be redistributed and even increased beyond the initial value, which does not exist in the two-qubit $\mathcal{PT}$-symmetric system. This phenomenon is related to the non-Hermiticity introduced on Alice, which triggers information exchange and leads to entanglement change in the Bob-Charlie subsystem. Some theoretical and numerical analyses are introduced to investigate the properties of the partial-information reserved quantum states in the broken phase of $\mathcal{PT}$ symmetry. By enlarging the system with ancillary qubits and encoding the subsystem with the non-Hermitian Hamiltonian with postselection, an experimental demonstration of the stable states in ADP is realized on a four-qubit quantum simulator based on a quantum circuit algorithm.

II. ENTROPY OF STABLE STATES

We focus on the dynamical features of a composite system consisting of three qubits, which is initialized as a Greenberger-Horne-Zeilinger (GHZ) state [28] $|\psi_0\rangle = (|000\rangle + |111\rangle)/\sqrt{2}$, and the reduced density matrix of each single qubit is $\rho_{\text{single}} = I/2$, which is the maximally mixed state. Then one of the qubits, such as Alice qubit, performs the local operation $U_A = e^{-i\hat{H}_{\mathcal{PT}}t}$ (set $\hbar = 1$) on her own system with a $\mathcal{PT}$-symmetric Hamiltonian

$$\hat{H}_{\mathcal{PT}} = s(\sigma_x + ir\sigma_z), \qquad (1)$$

where σ_i ($i = x, y, z$) represent the Pauli matrix. The parameter $s > 0$ represents the energy scale and $r > 0$ is the degree of non-Hermiticity. The $\mathcal{PT}$-symmetric Hamiltonian $\hat{H}_{\mathcal{PT}}$ satisfies $(\mathcal{PT})\hat{H}_{\mathcal{PT}}(\mathcal{PT})^{-1} = \hat{H}_{\mathcal{PT}}$, where the operator $\mathcal{P} = \sigma_x$, and $\mathcal{T}$ corresponds to complex conjugation. The energy gap of the Hamiltonian $w = 2s\sqrt{1 - r^2}$ will be real as long as $r < 1$, which means the $\mathcal{PT}$ symmetry is unbroken. The condition $r > 1$ will lead to a broken phase with a transition at the exceptional point $r_{ep} = 1$. The three-body Hamiltonian can be expressed as $\hat{H}_{\mathcal{PT}}^3 = \hat{H}_{\mathcal{PT}} \otimes I_B \otimes I_C$. The density matrix
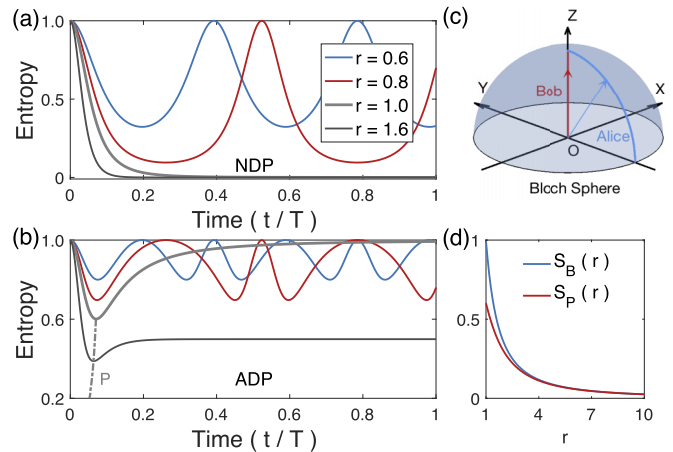

FIG. 2. Two kinds of dynamical evolution pattern. (a) The entropy $S(\rho_A)$ shows a NDP, while (b) $S(\rho_B)$ has an ADP. (c) Bloch vectors of Alice's and Bob's stable states labeled by lines with arrows in the Bloch upper hemisphere. Trajectory of Bloch vectors are represented by lines with corresponding colors when changing non-Hermiticity in a broken phase. (d) The entropy at point P and Bob's stable states.

$\rho(t)$ of the whole system can be obtained by a time-evolving operator with a renormalized quantum state [12],

$$\rho(t) = \frac{e^{-i\hat{H}_{\mathcal{PT}}^3 t} \rho(0) e^{i\hat{H}_{\mathcal{PT}}^{3\dagger} t}}{\text{tr}\left[e^{-i\hat{H}_{\mathcal{PT}}^3 t} \rho(0) e^{i\hat{H}_{\mathcal{PT}}^{3\dagger} t}\right]}. \qquad (2)$$

The joint reduced states of the two-body system are $\rho_{ij} = \text{tr}_k(\rho)$, while the single-body reduced density matrices are $\rho_i = \text{tr}_{jk}(\rho)$ ($i, j, k = A, B, C$). We focus on the dynamical features of the von Neumann entropy $S(\rho) = -\text{tr}(\rho \log_2 \rho)$ [1] and plot the evolution process within the total time T under different phases in Figs. 2(a) and 2(b). It can be concluded that in the triple-qubit $\mathcal{PT}$-symmetric system, for the single-body subsystem the entropy of Alice can still evolve under NDP: Entropy oscillates in the unbroken phase and the amplitude increases when the parameter r approaches r_{ep}. Once crossing the exceptional point, entropy exponentially decays to zero and the system tends to be stable states, which are indistinguishable in terms of entropy evolution characteristics. However, the dynamic pattern of $S(\rho_B)$ changed and another kind of ADP shows up in the Bob qubit: Entropy still oscillates in the unbroken phase, whereas in the broken phase of $\mathcal{PT}$ symmetry, the entropy of stable states will not decrease to zero exponentially but stabilizes to a value related to the degree of non-Hermiticity. In other words, there exists a parameter-dependent stable state in the subsystem of multiparty $\mathcal{PT}$-symmetric systems, and the entropy decreases with the increase of non-Hermiticity. Such a stable state can maintain partial entropy in the system under broken $\mathcal{PT}$ symmetry.

Based on the evolution equation, we can determine the reduced density matrix of qubit Bob,

$$\rho_B = \frac{1}{N}\begin{pmatrix} |C|^2 + (A - B)^2 & 0 \\ 0 & |C|^2 + (A + B)^2 \end{pmatrix}, \qquad (3)$$

where $A = \cos(wt/2)$, $B = (-2rs/w)\sin(wt/2)$, $C = (-2is/w)\sin(wt/2)$, and $N = 2(|C|^2 + A^2 + B^2)$ is the

normalization constant. We focus on the stable state in the broken phase with $\rho_B^{ss} = \frac{1}{2}I + \frac{\sqrt{r^2-1}}{2r}\sigma_z$. At the exceptional point, the density matrix of the stable state is a maximally mixed state with entropy $S(\rho_B) = 1$. However, with the increase of non-Hermiticity, the stable state will tend to be $\rho_B^{ss} = |0\rangle\langle 0|$, a pure state with entropy $S(\rho_B) = 0$. It can serve as a quantum state purification phenomenon induced by the non-Hermiticity increase, and the pure state is a stable state with time. Then we can calculate the analytical expression of the von Neumann entropy for the Bob qubit in ADP as follows:

$$S(\rho_B^{ss}) = \log_2 \frac{2}{\cos\theta(\sec\theta + \tan\theta)^{\sin\theta}} > 0, \qquad (4)$$

where $\cos\theta = 1/r$ and $\theta \in [0, \pi/2)$. The entropy will not be zero unless $\theta = \pi/2$, which means the non-Hermiticity of the system is infinity. Moreover, we plot the Bloch vectors of stable states of Bob in the Bloch sphere, just as in Fig. 2(c). The norm of the Bloch vector of Bob in stable states is $||\vec{r}_B|| = \sin\theta \leqslant 1$, which starts at the center of the Bloch sphere at the exceptional point and moves towards the top point with increasing non-Hermiticity.

As for the entropy evolution in NDP, the density matrix of Alice in a stable state with broken $\mathcal{PT}$ symmetry is $\rho_A^{ss} = \rho_B^{ss} - D(r)\sigma_y$. It can be found that the stable states of Alice and Bob have the same population distribution, but the ρ_A^{ss} has off-diagonal elements which decrease in power law with a damping function $D(r) = 1/(2r)$. Such effects can be modeled as a phase damping process induced by non-Hermiticity, leading to the loss of quantum information to the environment. When r increases from the exceptional point to a large enough value, the Bloch vector of Alice's stable state rotates along the Bloch sphere surface from point $(0, -1, 0)$ towards the north point of the z axis with norm $||\vec{r}_A|| = 1$ for all of the process. Therefore the entropy of the stable state in NDP is

$$S(\rho_A^{ss}) = -\sum_{i=1,2} \lambda_i^A \log_2 \lambda_i^A \equiv 0, \qquad (5)$$

with eigenvalues $\lambda_{1,2}^A = 0, 1$ which are not related to the non-Hermiticity parameter, and this is what happens in the evolution process obeying the NDP. Moreover, besides the stable states, there exists another kind of non-Hermiticity-related quantum state satisfying $dS(t)/dt = 0$ at the specific points $P = (t_P(r), S_P(r))$, labeled by gray dashed line in Fig. 2(b). During the evolution from point P to the stable state in ADP the entropy increases, and this turning point does not exist in NDP. With the increase of the non-Hermiticity parameter, the entropy of a quantum state at time point t_P will gradually approach $S(\rho_B^{ss})$, and the duration and intensity of the entropy increase process will gradually weaken until it disappears.

III. ENTANGLEMENT EVOLUTION

We now investigate the dynamical features of interaction and entanglement in the triple-party $\mathcal{PT}$-symmetric system. Entropic quantities are generally used to quantify correlations and for a two-body system with density matrix ρ_{ij}, the amount of information shared between the two parts can be characterized by the mutual information defined as $I(i : j) = S(\rho_i) + S(\rho_j) - S(\rho_{ij}) \geqslant 0$. The mutual information is always non-

negative and cannot be zero unless i and j are in a separable state, ensuring that $I(i : j)$ is a genuine measure of correlations [29]. It is usually believed that local trace-preserving quantum operations can never increase mutual information [1], but this can be violated in the two-qubit $\mathcal{PT}$-symmetric system without exceeding the initial value [11,13].

In the triple-qubit $\mathcal{PT}$-symmetric system, this property still can be held in the subsystem (Alice-Bob) under NDP, just as in Fig. 3(a). However, we find that evolution in the ADP of $I(B : C)$, which has nonzero mutual information in the broken phase, can present mutual information beyond the initial value. Moreover, the mutual information $I(B : C)$ oscillates with a maximum deviation I_{md} from the initial values at a series of discrete time points but tends to be stable at value I_s after passing the exceptional point. We define a variation measure $\Delta I(r) = \mathcal{O}(r_{ep} - r)I_{md} + \mathcal{O}(r - r_{ep})I_s - I(t_0)$ to quantify the increase of mutual information, where $\mathcal{O}(\cdot)$ is the Heaviside step function. We can conclude from Fig. 3(b) that the stable value I_s decreases with r and the subsystem (Bob-Charlie) has the maximal available information at the exceptional point. However, the increasing process of mutual information stops at $r_{MI} \approx 1.5978$, a critical point for increase of mutual information, which is different from the exceptional point of the $\mathcal{PT}$ symmetry. In other words, the critical point for transition of phase is not that for the increase of accessible information in triple-qubit $\mathcal{PT}$-symmetric systems. It is noted that there exists an anticorresponding relation between entropy and mutual information evolution because $I(B : C, t_\infty) = 2S(\rho_B^{ss})$: The two-body subsystems, which have NDP in entropy evolution, can present ADP in mutual information evolution and vice versa.

To evaluate the degree of entanglement in the two-body subsystem, we can also use concurrence [30],

$$C(\rho_{ij}) = \text{Max}\{0, \sqrt{\lambda_1} - \sqrt{\lambda_2} - \sqrt{\lambda_3} - \sqrt{\lambda_4}\}, \qquad (6)$$

where λ_i represents the eigenvalues of $\rho_{ij}(\sigma_y\sigma_y)\rho_{ij}^*(\sigma_y\sigma_y)$ in decreasing order. We numerically calculate the dynamical evolution and find that $C(\rho_{AB}) = C(\rho_{AC}) = 0$ all the time, which does not show evolution. It is Alice's $\mathcal{PT}$-symmetric operators that introduce the non-Hermiticity, but the systems including the Alice qubit do not show entanglement oscillation, and this is different from the two-qubit counterparts. For $C(\rho_{BC})$ the concurrence will emerge both in the unbroken and broken phases, although their local Hamiltonians are Hermitian. This evolution pattern is consistent with the entropic quantities of mutual information, which both present oscillation phenomenon in symmetry-unbroken phase while stabilizing at a non-Hermiticity-related nonzero value under broken $\mathcal{PT}$ symmetry. We identify the amplitude of concurrence during the evolution by $A(r) = C_{max}$, and it can be concluded from Fig. 3(c) that the concurrence of ρ_{BC}^{ss} will decrease and tend to be stable at $C_s = 1/r$, which presents a power-law decay with the increase of non-Hermiticity after the exceptional point.

IV. EXPERIMENTAL OBSERVATION OF STABLE STATES

In the experiment we focus on demonstrating the entropy dynamic evolution of stable states in the triple-qubit system with local $\mathcal{PT}$-symmetric operators on a liquid nuclear
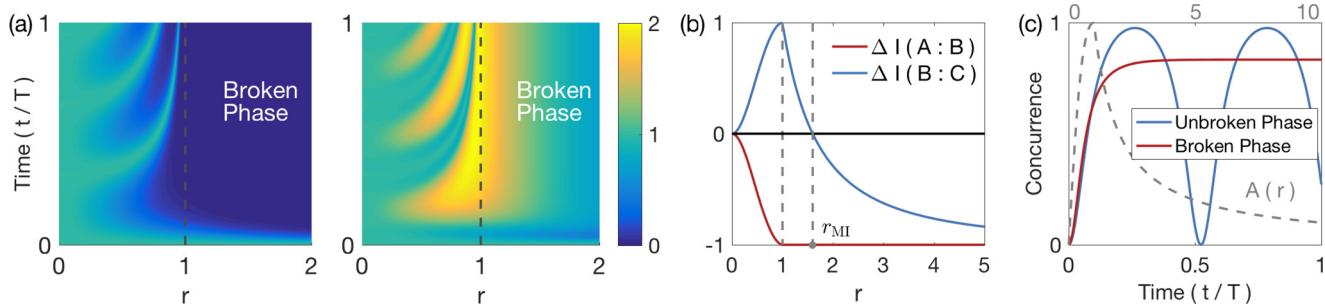
FIG. 3. (a) Mutual information of I($A : B$) (left) and I($B : C$) (right) with time under different non-Hermiticity. (b) Increase of mutual information ΔI($A : B$) and ΔI($B : C$) of stable states with the degree of non-Hermiticity. (c) Concurrence of two-body subsystem (Bob-Charlie) in the different $\mathcal{PT}$ phases. The gray dashed line is the amplitude of concurrence with non-Hermiticity whose range is shown on the top, while the other solid lines are concurrence evolution with time in an unbroken phase ($r = 0.8$) and broken phase ($r = 1.2$).

magnetic resonance quantum simulator. The sample used is ^{13}C-labeled iodotrifluoroethylene (C_2F_3I), and the qubits in the blue box of Fig. 4 encode the work system while another nucleus $^{19}F_3$ is chosen as an ancillary system to realize the $\mathcal{PT}$-symmetric operator [11]. The operators in the dotted box initialize the work system to the GHZ state. To realize the quantum simulation of the nonunitary evolution induced by $\mathcal{PT}$-symmetric Hamiltonian on Alice, we decompose the non-Hermitian Hamiltonian evolution into a linear combination of unitary operators and realize the simulation in an enlarged Hilbert space with postselection [31–34]. Notations H in the quantum circuit represent Hadamard gates and the 1-controlled gate $V_2 = \sigma_z$. The single-qubit operator V_0 and 0-controlled V_1 are parameter-dependent quantum gates, and the concrete forms are

$$V_0 = \begin{pmatrix} \cos\phi & -\sin\phi \\ \sin\phi & \cos\phi \end{pmatrix}, \quad V_1 = \begin{pmatrix} \cos\phi_1 & i\sin\phi_1 \\ i\sin\phi_1 & \cos\phi_1 \end{pmatrix}, \quad (7)$$

where $\phi = \arcsin\frac{r\sin(wt/2)}{M_1}$, $\phi_1 = \arcsin\frac{-\sin(wt/2)}{M_2}$ and $M_1 = [1 - r^2\cos wt]^{1/2}$, $M_2 = [1 - r^2\cos^2(wt/2)]^{1/2}$. Then the evolution can be realized via single-qubit operations and two-qubit controlled gates. We take several different parameter points in the experiment, and all the operations are realized using shaped pulses [35,36], while being robust to the static field distributions and inhomogeneity, and the durations of the experimental pulses are within 15 ms. At the end of quantum circuit, we obtain the density matrix of the work system by ob-

serving the probe spin ^{13}C in the subspace $|0\rangle$ of the ancillary qubit [37]. We trace out different qubits of the experimental stable states to find the subsystems with different dynamical patterns.

As shown in Fig. 5(a), the nondiagonal elements of the density matrix of Alice's stable states present a power-law decay with the increase of non-Hermiticity, which is consistent with the damping function $D(r)$. It is how quantum states behave in the NDP as analyzed above. In ADP we experimentally determine the entropy of Bob and concurrence between Bob and Charlie in Fig. 5(b), which both present the parameter-related nonzero value in stable states with broken $\mathcal{PT}$ symmetry. The experimental results of entropy match well with the theoretical expectation of Eq. (4) in different
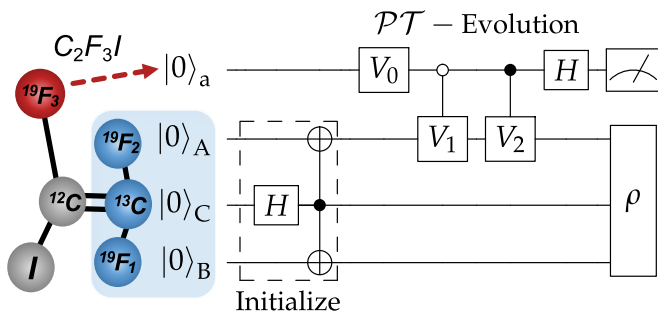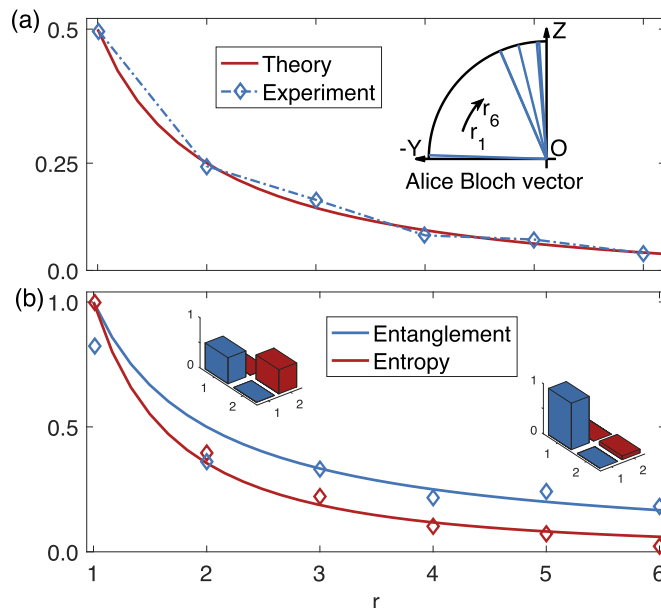

FIG. 4. Experimental sample and quantum circuit. Three of the four controllable qubits are used as a work system and the last one is an ancillary qubit. The whole process is divided into initial state preparation, $\mathcal{PT}$-symmetric evolution, and measurement.

FIG. 5. (a) The off-diagonal elements of stable states ρ_A^{ss} in the NDP. The diamond points are experimental results, while the solid line represents the theoretical expectations. The inset panel shows the experimentally identified Bloch vectors of Alice. (b) Experimental results of entropy and concurrence of the stable states in ADP. The inset panels represent the density matrices of Bob with minimal and maximal non-Hermiticity in the experimental parameter setup.

parameter conditions. The inset panels represent the density matrices of quantum states of Bob with minimal and maximal non-Hermiticity in an experimental parameter setup with average fidelities over 0.989, and we can see that with the increase of non-Hermiticity, ρ_B^{ss} gradually evolves from the maximally mixed state to a pure state.

V. CONCLUSION

We investigate the evolution process of entropy and entanglement in a triple-qubit system with local $\mathcal{PT}$-symmetric operation from theoretical and experimental perspectives. Two kinds of dynamic pattern, named ADP and NDP, are found in this system, where entropy and entanglement tend to be stable at a non-Hermiticity-related nonzero value in the ADP which does not exist in the two-qubit counterparts. Two-body subsystems in ADP present a maximum entanglement increase at the exceptional point, and mutual information can increase beyond the initial values. A new critical point r_{MI} is determined in the broken phase, where the transition of accessible information from increase to decrease compared with the initial condition happens. Based on the four-qubit quantum simulator, we experimentally observe the stable states in a non-Hermitian system with nuclear spins and the results confirmed the theoretical analysis. Our work shows that when the $\mathcal{PT}$-symmetric system is extended from two body to triple body, some different physical properties occur and the enhancement of entanglement and mutual information has important physical significance. Specifically, there are some potential applications in quantum communication and quantum eavesdropping by regulating and controlling the channel capacity of the system with local $\mathcal{PT}$-symmetric operators on the third party.

APPENDIX A: DERIVATION OF ENTROPY EVOLUTION OF STABLE STATES

In the triple-qubit system, the nonunitary operator on Alice induced by the $\mathcal{PT}$-symmetric Hamiltonian is

$$U_A = e^{i\phi}\begin{pmatrix} \cos\frac{wt}{2\hbar} + \frac{2rs}{w}\sin\frac{wt}{2\hbar} & \frac{-2is}{w}\sin\frac{wt}{2\hbar} \\ \frac{2is}{w}\sin\frac{wt}{2\hbar} & \cos\frac{wt}{2\hbar} - \frac{2rs}{w}\sin\frac{wt}{2\hbar} \end{pmatrix}, \quad (A1)$$

where ϕ is a phase factor. Because the triple-qubit Hamiltonian is a direct product of each single-body Hamiltonian, the operator on the whole system can be expressed as $U_3 = U_A \otimes$

$I_B \otimes I_C$. Then the time-dependent quantum state of the triple-qubit system without considering the normalization constant is $\rho(t) = U_3\rho(0)U_3^\dagger$. We need to trace out the other qubits to find the density matrix of Bob, which presents an ADP in entropy evolution and can be realized by

$$\rho_B(t) = \sum_{i,j=0,1} ((\langle i| \otimes I \otimes \langle j|)\rho(t)(|j\rangle \otimes I \otimes |i\rangle))$$

$$= \frac{1}{N}\begin{pmatrix} |C|^2 + (A-B)^2 & 0 \\ 0 & |C|^2 + (A+B)^2 \end{pmatrix}, \quad (A2)$$

where $A = \cos(wt/2\hbar)$, $B = (-2rs/w)\sin(wt/2\hbar)$, $C = (-2is/w)\sin(wt/2\hbar)$, and $N = 2(|C|^2 + A^2 + B^2)$ is the normalization constant. In the unbroken phase of the $\mathcal{PT}$ symmetry, each item in the quantum state oscillates with time periodically. However, when the symmetry is broken, the energy gap will become a pure imaginary number and we set $w/2\hbar = ik$, where k is a positive real number. According to the Euler equations, we can decompose each item in the quantum state into exponentially increasing item and exponentially decreasing item, where the latter can be abandoned in the long-time limit:

$$\lim_{t\to\infty}\begin{cases} \cos^2\frac{wt}{2\hbar} = e^{2kt}/4 \\ \sin^2\frac{wt}{2\hbar} = -e^{2kt}/4 \\ \cos\frac{wt}{2\hbar}\sin\frac{wt}{2\hbar} = ie^{2kt}/4 \end{cases}. \quad (A3)$$

Then the eigenvalues of the renormalized density matrix ρ_B^{ss} is $\lambda_{1,2}^B = \frac{r\pm\sqrt{r^2-1}}{2r}$, and we can calculate the analytical expression of the von Neumann entropy of the stable state in ADP,

$$S(\rho_B^{ss}) = -\sum_{i=1,2} \lambda_i^B \log_2 \lambda_i^B$$

$$= \log_2 2r - \frac{\sqrt{r^2-1}}{r}\log_2(r + \sqrt{r^2-1})$$

$$= \log_2 \frac{2}{\cos\theta(\sec\theta + \tan\theta)^{\sin\theta}}, \quad (A4)$$

where $\cos\theta = 1/r$ and $\theta \in [0, \pi/2)$. Based on the variable substitution, we can rewrite the quantum state as

$$\rho_B^{ss} = \frac{I + \sin\theta\sigma_z}{2}, \quad (A5)$$

and the Bloch vector is $\vec{r}_B = (0, 0, \sin\theta)$. So we can see that the purity of the stable state is parameter dependent, and the stable state will evolve from a maximally mixed state to a pure state $|0\rangle$ with increasing non-Hermiticity. However, when we turn to the quantum stable state of the Alice qubit, the density matrix have off-diagonal elements and the stable state in the broken phase is

$$\rho_A^{ss} = \lim_{t\to\infty} \frac{1}{N}\begin{pmatrix} |C|^2 + (A-B)^2 & 2BC \\ -2BC & |C|^2 + (A+B)^2 \end{pmatrix}$$

$$= \begin{pmatrix} \frac{r+\sqrt{r^2-1}}{2r} & \frac{-i}{2r} \\ \frac{i}{2r} & \frac{r-\sqrt{r^2-1}}{2r} \end{pmatrix}$$

$$= \frac{I - \cos\theta\sigma_y + \sin\theta\sigma_z}{2}, \quad (A6)$$

where the damping function $D(r) = \cos\theta/2 = 1/2r$ and the norm of the Bloch vector is $||\vec{r}_A|| = \cos^2\theta + \sin^2\theta = 1$, which is parameter independent. The eigenvalues of the stable state of Alice are

$$
\begin{aligned}
\lambda_{1,2}^A &= \frac{\rho_{A(11)}^{ss} + \rho_{A(22)}^{ss}}{2} \pm \\
&\quad \frac{\sqrt{\left(\rho_{A(11)}^{ss} - \rho_{A(22)}^{ss}\right)^2 + 4\rho_{A(12)}^{ss}\rho_{A(21)}^{ss}}}{2} \\
&= \frac{1 \pm \sqrt{(r^2-1)/r^2 + 1/r^2}}{2} \\
&= 0, 1,
\end{aligned} \tag{A7}
$$

and this results that the entropy of stable states in the NDP stays zero all the time and is parameter independent. This leads to the fact that in the broken phase, the mutual information of subsystem Bob and Charlie is $I(B:C, t \to \infty) = S(\rho_B^{ss}) + S(\rho_C^{ss}) - S(\rho_{BC}^{ss}) = 2S(\rho_B^{ss})$. So by numerically solving the equation $S(\rho_B^{ss}) = 1/2$, we can determine the critical point r_{MI} in the broken phase.

APPENDIX B: EXPERIMENTAL SIMULATION OF THE STABLE STATES

1. Initialization

The experiments for simulating the stable states in a triple-qubit system with local $\mathcal{PT}$-symmetric operator are carried out on a 600-MHz nuclear magnetic resonance platform at room temperature (298 K) with a four-qubit sample ^{13}C-labeled iodotrifluoroethylene dissolved in d-chloroform. The spectrometer is equipped with a superconducting magnet which creates a strong magnetic field (14.1T). The sample is placed in the static magnetic field along the z direction, and the internal Hamiltonian under the weak-coupling approximation is

$$
H_{\text{int}} = -\sum_{i=1}^{4} \pi \nu_i \sigma_z^i + \sum_{i<j}^{4} \frac{\pi}{2} J_{ij} \sigma_z^i \sigma_z^j, \tag{B1}
$$

	Q1	Q2	Q3	Q4
Q1	-23212.5			
Q2	-297.9	49537.1		
Q3	-275.5	64.3	63904.5	
Q4	39.2	51.2	-128.9	84619.8
Spins	^{13}C	$^{19}F_1$	$^{19}F_2$	$^{19}F_3$
T2(s)	3.3	2.7	2.6	2.7

FIG. 6. Molecule structure and molecule parameters of the sample. ^{13}C, $^{19}F_1$, $^{19}F_2$, and $^{19}F_3$ are used as four qubits in the experiment. The chemical shifts and J couplings (in units of Hz) are listed by the diagonal and off-diagonal elements, respectively. The transversal relaxation times T2 (in seconds) are also shown at the bottom.
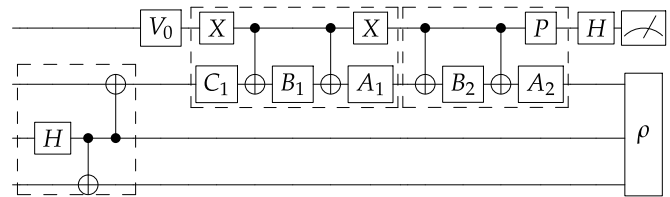

FIG. 7. Quantum gate decomposition for the simulation of the triple-qubit system with local $\mathcal{PT}$-symmetric operator. The concrete forms of the single-qubit gates are shown in Table I.

where ν_i is the chemical shift and J_{ij} is the J-coupling strength between the ith and jth nuclei. The experimentally identified parameters of this molecule are shown in Fig. 6. The initialization process of quantum computation in the liquid nuclear magnetic resonance system starts from a thermal equilibrium state obeying Boltzmann distribution:

$$
\rho_{\text{eq}} = \frac{e^{-H_{\text{int}}/k_B T}}{\text{tr}(e^{-H_{\text{int}}/k_B T})}, \tag{B2}
$$

where k_B is the Boltzmann constant and T is the thermodynamic temperature. Under the condition that $\|H_{\text{int}}/k_B T\| \ll 1$ and $J_{kl} \ll \omega_i$, the thermal equilibrium state in our platform can be approximated as

$$
\rho_{\text{eq}} \approx \frac{1}{2^4} \left(I^{\otimes 4} + \sum_i^4 \frac{\hbar w_i \sigma_z^i}{2 k_B T} \right), \tag{B3}
$$

where the notation I is the identity matrix and σ_z is a Pauli matrix. To initialize the system, we generally need to drive the quantum system from the highly mixed state ρ_{eq}, which can not be used as an initial state to the pseudopure state (PPS),

$$
|\rho_{\text{pps}}\rangle = \frac{1-\epsilon}{2^4} I^{\otimes 4} + \epsilon |0000\rangle\langle 0000|, \tag{B4}
$$

where $\epsilon \approx 10^{-5}$ is polarization. The first term can be neglected, since the identity matrix does not evolve under any unitary propagator and cannot be observed. We prepared the PPS from the thermal equilibrium state with the selective-transition method [37,38], which is realized by unitary operators and field gradient pulses in the z direction (Gz). The unitary operators redistribute the diagonal elements, and the Gz pulse is used to eliminate the undesired coherence, except the zero-quantum coherence of spins. After these processes the PPS is prepared, and this state serves as the starting point for subsequent computation tasks.

TABLE I. Decomposition scheme of quantum algorithm with single-qubit gates and CNOT gate according to the parameter setting in experiment. The $R_i(\alpha)$ ($i = y, z$) is a rotation operator along the i axis with angle α.

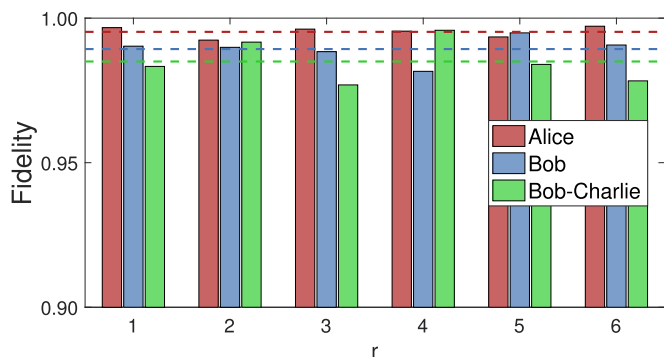|		
A_1: $R_z(1.5\pi)R_y(\phi_1)$	A_2: $R_z(1.5\pi)R_y(\pi)$	V_0: $R_y(0.5\pi)$
B_1: $R_y(-\phi_1)R_z(-\pi)$	B_2: $R_y(-\pi)R_z(-1.5\pi)$	P: $\begin{pmatrix} 1 & 0 \\ 0 & -i \end{pmatrix}$
C_1: $R_z(-0.5\pi)$	X: $R_z(-0.5\pi)R_y(\pi)R_z(0.5\pi)$	

FIG. 8. Fidelities of subsystems between the experimental stable states and the theoretical expectations under different non-Hermiticity. The average fidelities are labeled by lines with corresponding colors.

2. Quantum Simulation of $\mathcal{PT}$-Symmetric Operator

To realize the simulation of a nonunitary dynamical process induced by $\mathcal{PT}$-symmetric Hamiltonian, we encode the nonunitary evolution into a unitary process by adding an ancillary qubit and form a gate-based quantum circuit, which is friendly for experimentation. It is called a linear combination of unitaries, which is a universal subroutine in designing and developing quantum algorithms [31]. We first create superposition states on the ancillary system and then perform controlled operations on the work system. The physical picture is that different unitary operations are implemented simultaneously on the work system but in different subspaces, and the final results can be obtained in a specific subspace of ancillary systems according to the practical algorithm design.

Specifically, suppose that the operator for creating superposition states is $V_0 = [\cos\phi, -\sin\phi; \sin\phi, \cos\phi]$ and the nonunitary evolution operator can be decomposed into the

form $U_A = \cos\phi V_1 + \sin\phi V_2$, where

$$V_1 = \begin{pmatrix} \cos\phi_1 & i\sin\phi_1 \\ i\sin\phi_1 & \cos\phi_1 \end{pmatrix}, \quad V_2 = \begin{pmatrix} \cos\phi_2 & -i\sin\phi_2 \\ i\sin\phi_2 & -\cos\phi_2 \end{pmatrix}.$$

(B5)

Under the unitary limitation on V_i ($i = 0, 1, 2$), the choice of these operators is not unique. This construction leads to four equations as follows:

$$\cos\phi \cos\phi_1 = \cos\frac{wt}{2\hbar}$$

$$\sin\phi \cos\phi_2 = \frac{2rs}{w}\sin\frac{wt}{2\hbar}$$

$$\cos\phi \sin\phi_1 = \frac{-2s}{w}\sin\frac{wt}{2\hbar}$$

$$\sin\phi \sin\phi_2 = 0.$$

(B6)

By solving these equations, we can determine the angles ϕ and $\phi_{1,2}$ as shown in the main text. It worth noting that $\tan\phi_2 = 0$, and this leads to $V_2 = \sigma_z$. Single-qubit operator V_0 and two-qubit operator V_1 are parameter-dependent quantum gates, while the other unitary quantum gates do not vary with the parameters in the $\mathcal{PT}$-symmetric Hamiltonian. In the broken phase of $\mathcal{PT}$ symmetry, the operators can be determined based on the experimental parameter setup and decomposed into single-qubit operations and controlled-NOT (CNOT) gates, as shown in Fig. 7. Quantum evolution according to the quantum circuit we constructed is optimized by gradient-ascent pulse engineering [35,36]. Each shaped pulse is simulated to be over 99.5% fidelity [39] while being robust to the static field distributions and inhomogeneity, and the durations of the experimental pulses are within 15 ms.

3. Measurement and Results

After the entanglement creation and $\mathcal{PT}$-symmetric evolution, quantum measurement is performed on a bulk ensemble
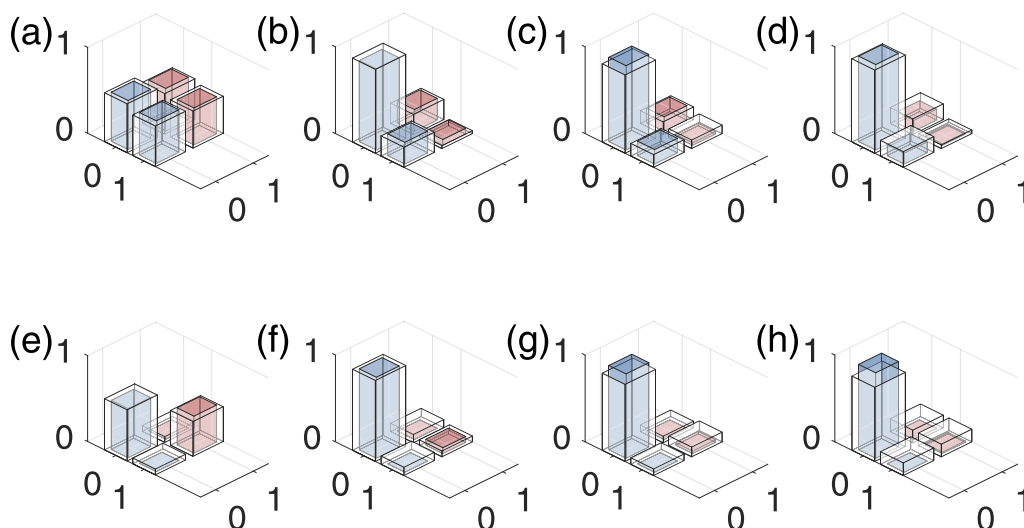

FIG. 9. The experimentally identified density matrix of stable states under different degrees of non-Hermiticity. Figures in the first row from (a) to (d) represent the quantum state of Alice in NDP ($r_1 \rightarrow r_4$), while figures in the second row from (e) to (h) show the density matrix of Bob in ADP. The external transparent bars represent the experimental results, while the internal solid bars represent the corresponding theoretical values of the density matrices. The quantum states are taken as absolute values for better display.

of molecules, which means the readout is an ensemble-averaged macroscopic measurement. At the end of the quantum circuit, all experimental data are extracted from the free-induction decay (FID), which is the signal induced by the precessing magnetization of the sample in a surrounding detection coil. The signal is then subjected to Fourier transformation, and the resulting spectral lines are fitted, yielding a set of measurement data. As the precession frequencies of different spins are distinguishable, they can be individually detected and all the observations are made on the probe spin ^{13}C [37]. By fitting the ^{13}C spectrum, the real parts and the imaginary parts of the peaks are extracted, which correspond to $\langle \hat{\sigma}_1^x \rangle$ and $\langle \hat{\sigma}_1^y \rangle$, respectively. Then we can reconstruct all the density matrix elements in the subspace where the ancillary qubit is $|0\rangle$ to get the target stable states of the triple-qubit work system under different experimental parameter setup. We plot the fidelities of different subsystems between the experimental results and theoretical expectations in Fig. 8 with average fidelities over 0.98. The corresponding density matrices of stable states, which evolve under NDP and ADP, respectively, are shown in Fig. 9, and both of them present a quantum state purification phenomenon with the increase of non-Hermiticity.

[1] M. A. Nielsen and I. L. Chuang, *Quantum Computation and Quantum Information: 10th Anniversary Edition*, 10th ed. (Cambridge University Press, New York, 2011).

[2] C. M. Bender and S. Boettcher, Real Spectra in Non-Hermitian Hamiltonians Having $\mathcal{PT}$ Symmetry, Phys. Rev. Lett. **80**, 5243 (1998).

[3] V. V. Konotop, J. Yang, and D. A. Zezyulin, Nonlinear waves in $\mathcal{PT}$-symmetric systems, Rev. Mod. Phys. **88**, 035002 (2016).

[4] R. El-Ganainy, K. G. Makris, M. Khajavikhan, Z. H. Musslimani, S. Rotter, and D. N. Christodoulides, Non-Hermitian physics and $\mathcal{PT}$ symmetry, Nat. Phys. **14**, 11 (2018).

[5] T. J. Milburn, J. Doppler, C. A. Holmes, S. Portolan, S. Rotter, and P. Rabl, General description of quasiadiabatic dynamical phenomena near exceptional points, Phys. Rev. A **92**, 052124 (2015).

[6] D. Heiss, Circling exceptional points, Nat. Phys. **12**, 823 (2016).

[7] C. M. Bender, D. C. Brody, H. F. Jones, and B. K. Meister, Faster than Hermitian Quantum Mechanics, Phys. Rev. Lett. **98**, 040403 (2007).

[8] Y.-C. Lee, M.-H. Hsieh, S. T. Flammia, and R.-K. Lee, Local $\mathcal{PT}$ Symmetry Violates the No-Signaling Principle, Phys. Rev. Lett. **112**, 130404 (2014).

[9] J.-S. Tang, Y. T. Wang, S. Yu, D. Y. He, J. S. Xu, B. H. Liu, G. Chen, Y. N. Sun, K. Sun, Y. J. Han, C.-F. Li, and G.-C. Guo, Experimental investigation of the no-signalling principle in parity-time symmetric theory using an open quantum system, Nat. Photon. **10**, 642 (2016).

[10] S.-L. Chen, G.-Y. Chen, and Y.-N. Chen, Increase of entanglement by local $\mathcal{PT}$-symmetric operations, Phys. Rev. A **90**, 054301 (2014).

[11] J.-W. Wen, C. Zheng, X.-Y. Kong, S.-J. Wei, T. Xin, and G.-L. Long, Experimental demonstration of a digital quantum simulation of a general $\mathcal{PT}$-symmetric system, Phys. Rev. A **99**, 062122 (2019).

[12] K. Kawabata, Y. Ashida, and M. Ueda, Information Retrieval and Criticality in Parity-Time-Symmetric Systems, Phys. Rev. Lett. **119**, 190401 (2017).

[13] L. Xiao, K.-K. Wang, X. Zhan, Z.-H. Bian, K. Kawabata, M. Ueda, W. Yi, and P. Xue, Observation of Critical Phenomena in Parity-Time-Symmetric Quantum Dynamics, Phys. Rev. Lett. **123**, 230401 (2019).

[14] C. M. Bender, D. C. Brody, and H. F. Jones, Complex Extension of Quantum Mechanics, Phys. Rev. Lett. **89**, 270401 (2002).

[15] C. M. Bender, D. W. Hook, P. N. Meisinger, and Q.-H. Wang, Complex Correspondence Principle, Phys. Rev. Lett. **104**, 061601 (2010).

[16] S. Croke, $\mathcal{PT}$-symmetric Hamiltonians and their application in quantum information, Phys. Rev. A **91**, 052113 (2015).

[17] C.-Y. Ju, A. Miranowicz, G.-Y. Chen, and F. Nori, Non-Hermitian Hamiltonians and no-go theorems in quantum information, Phys. Rev. A **100**, 062118 (2019).

[18] J. Li, A. K. Harter, J. Liu, L. de Melo, Y. N. Joglekar, and L. Luo, Observation of parity-time symmetry breaking transitions in a dissipative Floquet system of ultracold atoms, Nat. Commun. **10**, 855 (2019).

[19] Y. Wu, W. Liu, J. Geng, X. Song, X. Ye, C.-K. Duan, X. Rong, and J. Du, Observation of parity-time symmetry breaking in a single-spin system, Science **364**, 878 (2019).

[20] A. Guo, G. J. Salamo, D. Duchesne, R. Morandotti, M. Volatier-Ravat, V. Aimez, G. A. Siviloglou, and D. N. Christodoulides, Observation of $\mathcal{PT}$-Symmetry Breaking in Complex Optical Potentials, Phys. Rev. Lett. **103**, 093902 (2009).

[21] C. E. Ruter, K. G. Makris, R. El-Ganainy, D. N. Christodoulides, M. Segev, and D. Kip, Observation of parity-time symmetry in optics, Nat. Phys. **6**, 192 (2010).

[22] C. M. Bender, B. K. Berntson, D. Parker, and E. Samuel, Observation of $\mathcal{PT}$ phase transition in a simple mechanical system, Am. J. Phys. **81**, 173 (2013).

[23] M. Naghiloo, M. Abbasi, Y. N. Joglekar, and K. W. Murch, Quantum state tomography across the exceptional point in a single dissipative qubit, Nat. Phys. **15**, 1232 (2019).

[24] K. Ding, G. Ma, Z. Q. Zhang, and C. T. Chan, Experimental Demonstration of an Anisotropic Exceptional Point, Phys. Rev. Lett. **121**, 085702 (2018).

[25] L. Xiao, X. Zhan, Z. H. Bian, K. K. Wang, X. Zhang, X. P. Wang, J. Li, K. Mochizuki, D. Kim, N. Kawakami, W. Yi, H. Obuse, B. C. Sanders, and P. Xue, Observation of topological edge states in parity-time-symmetric quantum walks, Nat. Phys. **13**, 1117 (2017).

[26] S. Weimann, M. Kremer, Y. Plotnik, Y. Lumer, S. Nolte, K. G. Makris, M. Segev, M. C. Rechtsman, and A. Szameit, Topologically protected bound states in photonic parity-time-symmetric crystals, Nat. Mater. **16**, 433 (2017).

[27] C. Zheng, L. Hao, and G. L. Long, Observation of a fast evolution in a parity-time-symmetric system, Philos. Trans. R. Soc. A **371**, 20120053 (2013).

[28] D. M. Greenberger, M. A. Horne, A. Shimony, and A. Zeilinger, Bell's theorem without inequalities, Am. J. Phys. **58**, 1131 (1990).

[29] G. Camilo, G. T. Landi, and S. Eliëns, Strong subadditivity of the Rényi entropies for bosonic and fermionic Gaussian states, Phys. Rev. B **99**, 045155 (2019).

[30] W. K. Wootters, Entanglement of Formation of an Arbitrary State of Two Qubits, Phys. Rev. Lett. **80**, 2245 (1998).

[31] G. L. Long, General quantum interference principle and duality computer, Commun. Theor. Phys. **45**, 825 (2006).

[32] U. Gunther and B. F. Samsonov, Naimark-Dilated $\mathcal{PT}$-Symmetric Brachistochrone, Phys. Rev. Lett. **101**, 230404 (2008).

[33] M.-Y. Huang, R.-K. Lee, L.-J. Zhang, S.-M. Fei, and J.-D. Wu, Simulating Broken $\mathcal{PT}$-Symmetric Hamiltonian Systems by Weak Measurement, Phys. Rev. Lett. **123**, 080404 (2019).

[34] C. Zheng, Duality quantum simulation of a general parity-time-symmetric two-level system, Europhys. Lett. **123**, 40002 (2018).

[35] N. Khaneja, T. Reiss, C. Kehlet, T. Schulte-Herbruggen, and S. J. Glaser, Optimal control of coupled spin dynamics: Design of NMR pulse sequences by gradient ascent algorithms, J. Magn. Reson. **172**, 296 (2005).

[36] C. A. Ryan, C. Negrevergne, M. Laforest, E. Knill, and R. Laflamme, Liquid-state nuclear magnetic resonance as a testbed for developing quantum control methods, Phys. Rev. A **78**, 012328 (2008).

[37] H. Wang, S. Wei, C. Zheng, X. Kong, J. Wen, X. Nie, J. Li, D. Lu, and T. Xin, Experimental simulation of the four-dimensional Yang-Baxter equation on a spin quantum simulator, Phys. Rev. A **102**, 012610 (2020).

[38] X. Peng, X. Zhu, X. Fang, M. Feng, K. Gao, X. Yang, and M. Liu, Preparation of pseudo-pure states by line-selective pulses in nuclear magnetic resonance, Chem. Phys. Lett. **340**, 509 (2001).

[39] E. M. Fortunato, M. A. Pravia, N. Boulant, G. Teklemariam, T. F. Havel, and D. G. Cory, Design of strongly modulating pulses to implement precise effective Hamiltonians for quantum information processing, J. Chem. Phys. **116**, 7599 (2002).